

Giant magnetoresistance in the variable range hopping regime

L. Ioffe

*LPTHE, Universite Pierre and Marie Curie, Boite 126, T13-14 4eme etage,
4 place Jussieu, Paris CEDEX 05, France and Department of Physics,
Rutgers University 136 Frelinghuysen Rd, Piscataway, New Jersey 08854 USA*

B.Spivak

Department of Physics, University of Washington, Seattle WA 98195, USA

We predict the universal power law dependence of localization length on magnetic field in the strongly localized regime. This effect is due to the orbital quantum interference. Physically, this dependence shows up in an anomalously large negative magnetoresistance in the hopping regime. The reason for the universality is that the problem of the electron tunneling in a random media belongs to the same universality class as directed polymer problem even in the case of wave functions of random sign. We present numerical simulations which prove this conjecture. We discuss the existing experiments that show anomalously large magnetoresistance. We also discuss the role of localized spins in real materials and the spin polarizing effect of magnetic field.

I. INTRODUCTION

In strongly disordered conductors, single electrons states are localized, so the conductivity is due to phonon assisted electron tunneling between localized states. The length of a typical hop r_{hop} grows as temperature is decreased and becomes much larger than the distance between the localized states in the variable range hopping regime. [1, 2] In this paper we study the orbital mechanism of the magnetoresistance in this regime. We show that at sufficiently low temperatures it is due to the localization length dependence on magnetic field, B , and that it is given by a universal power law. This localization length dependence on magnetic field translates into an exponentially large variation of the resistance. The sign of the orbital magnetoresistance depends on the details of impurity scattering, but in the typical case the low temperature magnetoresistance is negative. Similar to the metallic regime, the origin of the negative magnetoresistance is the electron quantum interference, however, the amplitudes that interfere correspond to different processes in these two cases. Despite its much larger magnitude the negative magnetoresistance in the hopping regime received much less attention, both theoretically and experimentally, than its counterpart in the metallic regime. One of goals of this paper is to draw the attention of the community to this interesting phenomenon.

We begin with a brief review of the nature of the magnetoresistance in metals. The conventional theory of magnetoresistance associates it with the classical effect of electron motion along cyclotron orbits. For a typical metal the magnetoresistance is controlled by the parameter $(\omega_c \tau_{tr})^2$. Here ω_c is the cyclotron frequency, and τ_{tr} is the transport mean free time, (see e.g. [3]). In contrast to these expectations, many disordered metals show negative magnetoresistance at small magnetic fields. The negative magnetoresistance in weakly disordered metals has been explained in the framework of the weak localization theory, which takes into account the quantum interference of probability amplitudes for electrons to travel along self-intersecting diffusive paths [4–7] such as shown in the Fig. 1a. The interfering amplitudes correspond to the clockwise and counterclockwise propagation of the electron wave along the loop formed by the self-intersecting path. In the absence of magnetic field these amplitudes interfere constructively increasing the probability of return to the intersection point. In the presence of magnetic field these amplitudes acquire different phases, and the interference is suppressed leading to the negative magnetoresistance. The magnitude of negative magnetoresistance in this regime is relatively small because it scales with the small parameter $1/k_F l_{tr}$. Here k_F is the Fermi momentum, and l_{tr} is the transport mean free path.

Experimentally, in many materials the magnetoresistance in the hopping regime is significantly larger than in the metallic regime. A positive magnetoresistance of several orders of magnitude in hopping regime has been observed long ago (see, e.g. Ref. [1] and references therein). Significant negative magnetoresistance in variable range hopping regime ranging up to two orders of magnitude, has been observed in many experimental works [8–18]. In some of these works a large anisotropy of the negative magnetoresistance has been observed in 2D samples, indicating its orbital nature.

Phonon emission and absorption make different hopping events incoherent, whilst the electron tunneling between the localized states is a quantum mechanical process. The magnetoresistance is due to the magnetic field dependence of the probability of one hop. Qualitatively, large orbital magnetoresistance in the hopping regime is due the interference of the tunneling amplitudes along different tunneling paths contributing to a single hop that are distributed in a cigar-shaped region shown in 1b. In this regime the tunneling paths containing loops give exponentially small contribution to the tunneling probability. This is the main difference from the weak localization where the interference is due to

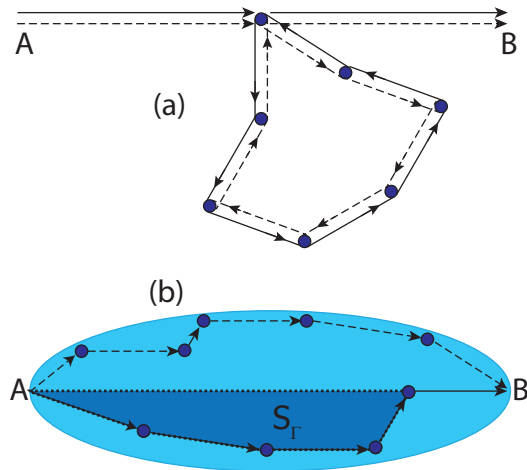


FIG. 1: Qualitative picture of the interference effects in disordered metals. Panel (a) shows interference in the weak localization regime that is due to self-crossing diffusive paths. Quantum propagation from A to B is the sum of two amplitudes that contain clockwise and counterclockwise motion along the loop that is a part of the self intersecting path. Panel (b) shows interference in hopping regime in which the backward motion of electrons gives negligible contribution to the tunneling between sites A and B. In this case typical paths contributing to the interference are located in the shaded (light blue) area with transverse direction that scales with the length of the hop, L . The magnetic field has a significant effect if the flux trough the area, S_r , formed by a typical path and a straight line (dark blue) is of the order of one flux quantum.

the paths that circle a loop (see 1a). Because in the variable range hopping regime electrons hop over distances much larger than the distance between localized states, the cigar-shaped region contains many electron scatterers. The amplitudes, μ_i , describing individual scattering process at state i may be positive and negative. The sign distribution of μ_i determines the sign of the magnetoresistance, as we explain below in section II C.

Large positive magnetoresistance may be associated with a shrinkage of the hydrogen-like localized electron wave functions at the scales less than the inter-impurity distance. Quantitatively this picture works well only in a very high magnetic field and at sufficiently high temperatures at which the typical electron hopping length is shorter than the distance between impurities. A theory of the positive magnetoresistance which takes into account the electron scattering with positive scattering amplitudes has been developed in works [19–23]. In this case the tunneling amplitudes interfere constructively in the absence of the field, while the phases induced by the magnetic field destroy this interference.

An orbital mechanism of the negative magnetoresistance may be associated with the randomness of the signs of the scattering amplitudes, μ_i , that is due to random sign of $\epsilon - \epsilon_i$. [24–29] Here ϵ is the energy of the tunneling electron and ϵ_i is the energy of a localized state. This sign randomness may lead to random signs of the interfering tunneling amplitudes at $B = 0$. The magnetic field makes tunneling amplitudes complex which increases the conductance in this situation. Thus, the sign of the orbital magnetoresistance is related to the sign distribution of the localized electron wave functions.

In this work we develop a quantitative theory of the orbital magnetoresistance in the hopping regime and discuss the available experimental data in the light of our results. Because most of experiments have been done on two dimensional samples we will focus on the two dimensional hopping regime of the electrons and corresponding experiments.

We show that for physically relevant cases even a small concentration of impurities with $\mu_i < 0$ leads to completely random signs of the tunneling amplitudes at large scales. Therefore, at sufficiently low temperatures and small magnetic field the variable range hopping magnetoresistance is negative. At higher magnetic field and higher temperatures it can be both positive and negative.

The plan of the paper is as follows: In section II A we start with a brief review of the basis of variable range hopping theory, and discuss qualitative picture of the variable range hopping magnetoresistance. In sections II B , II C we discuss the statistics of the modulus and of the sign of the localized electron wave function. In particular, in section II C we discuss the conditions for the existence of the “sign phase transition” where, as a function of the concentration of scatterers with $\mu_i < 0$, the system changes from the sign ordered to sign disordered phases. In section III we apply the theory developed in section II to compute the magnetoresistance. The section IV discusses applications of the results for the sign phase transition to other physical systems. Finally, section V gives a short review of the experimental situation.

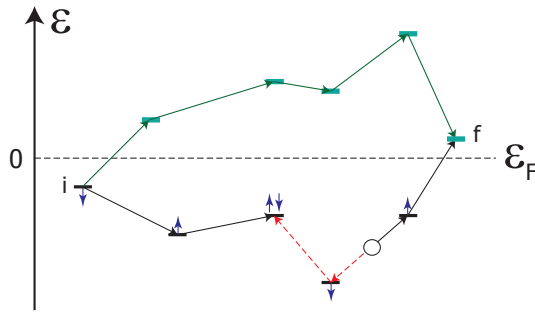


FIG. 2: Qualitative picture of the phonon assisted tunneling through localized states from the initial state i to the final state f . Solid bars indicate the energies of the localized states. The energies of the initial and final states are close to the Fermi energy $\epsilon_F = 0$ (indicated by the dashed line) whilst the intermediate localized states are typically further away from $\epsilon = 0$. The states with negative energies can be filled with one or two electrons. In the former case they are characterized by the spin of the electron shown by vertical arrows. The states with $\epsilon > 0$ are empty. Black and green (gray) arrows indicate electron tunneling paths through empty and filled localized states. If the path goes through the site that is already occupied by the electron with the same spin, the coherent process happens by creating an electron hole pair (indicated by empty circle), then by tunneling hole carrying the opposite spin in the opposite direction and finally by annihilating it with the electron coming from the left. This process leaves the spin state intact. The incoherent process in which the hole carrying the same spin might be also possible in some physical situations (see section III C).

II. ELECTRON TRANSPORT IN VARIABLE RANGE HOPPING REGIME.

A. Review of variable range hopping theory.

In the localized regime the electron wave functions decay exponentially with the distance, $|\mathbf{r} - \mathbf{r}_i|$, from the impurity: $\psi_i(\mathbf{r}) \sim \exp(-|\mathbf{r} - \mathbf{r}_i|/\xi)$ where \mathbf{r}_i is the center of the localized wave function and ξ is a typical localization radius. In this case the conductivity is determined by phonon assisted electron hopping between localized states. At low temperatures the typical hopping length r_{hop} is determined by the competition between two exponential factors: the hopping probability W_{ij} that decays exponentially with the distance between impurities r_{ij} and the thermal factor, $\exp(-E_{hop}(r_{ij})/T)$ where $E_{hop}(r_{ij})$ is the hopping activation energy that decreases with r_{ij} . These factors give the exponential dependence of the typical hopping rate at distance r_{hop} : $\exp(-E_{hop}(r)/T - 2r/\xi)$. This exponential factor is maximal for the typical hopping length, r_{hop} , which is much larger than the distance between localized states, as illustrated in Fig. 1b:

$$r_{hop} \sim \left(\frac{T_0}{T}\right)^\zeta \xi, \quad (1)$$

As a result, the resistivity acquires exponential dependence on temperature [1, 2]:

$$\rho(T) = \rho_o \exp[-(\frac{T_0}{T})^\zeta] \quad (2)$$

Here the prefactor ρ_o is determined by the electron-phonon matrix element, ξ is the localization radius.

Generally, the density of localized states can be energy dependent close to the Fermi energy [1]:

$$\nu(\epsilon) = C\epsilon^\beta. \quad (3)$$

where we count the energy, ϵ , of a tunneling electron from the Fermi energy. In the absence of electron-electron interaction (Mott's theory) the density of states at the Fermi level is constant ($\beta = 0$, $C = \nu_0$) leading to activation energy $T_0 \approx 13(\nu_0\xi^2)^{-1}$ and exponent $\zeta = 1/3$ for $d = 2$ (Mott law). In the case when electrons (in 2D or 3D) interact via three dimensional Coulomb interaction (Efros-Shklovskii regime) $\beta = 1$, $C \approx (2/\pi) e^4/\kappa^2$, where κ is the dielectric constant. This results in $\zeta = 1/2$, $T_0 \sim e^2/\kappa\xi$ for 2D electrons interacting via three dimensional Coulomb.

The qualitative arguments of the Mott theory can be made more quantitative by considering the optimal percolating cluster of electron hops.[1] Probability of a single hop between the states localized around positions r_i and r_j is given

by

$$W_{ij} = \frac{2\pi}{h} \int |M_{ij}(\vec{q})|^2 \delta(\epsilon_i - \epsilon_j - uq) d^d d \quad (4)$$

Here

$$M_{ij} \sim \int d^d r \psi_i(\vec{r} - \vec{r}_i) \psi_j(\vec{r} - \vec{r}_j) e^{i\vec{q}\vec{r}} \quad (5)$$

is the phonon matrix element, u is the speed of the sound and \vec{q} is its wave vector. Because the wave functions $\psi_i(\vec{r} - \vec{r}_i)$ and $\psi_j(\vec{r} - \vec{r}_j)$ decrease exponentially, M_{ij} and W_{ij} are exponential functions of the localization length, $\xi(B)$.

In the main part of our paper we consider the range of magnetic field in which $W_{ij}(B)$ dependence is dominated by $\xi(B)$. In this case one can approximate the phonon tunneling matrix element by the amplitude of tunneling between states i and j : $M_{ij} \sim A_{ij}$.

In the uniform medium the magnetic field suppresses the amplitude of a single quantum tunneling event:

$$A_{ij} \propto \exp(-r_{ij}^2/2L_B^2) \text{ at } r_{ij} \gg L_B^2/\xi \quad (6)$$

which gives positive magnetoresistance. Here $L_B = (c\hbar/eB)^{1/2}$ is the magnetic length. In disordered media, electrons scatter from other localized states which have energies different from the energy of the final state. The effect of magnetic field is due to the interference of the directed optimal paths, which is shown schematically in Fig. 1b. In this case $A_{if} = \sum_{\Gamma} A_{\Gamma}$ is a coherent sum of amplitudes, $A_{\Gamma}(B)$, to tunnel along paths Γ , between the initial "i" and final "f" sites. The tunneling paths can be defined by the sequence of states which scatter electrons in the course of tunneling. At zero magnetic field $\mathbf{B} = 0$ the wave functions of localized states and the tunneling amplitudes $A_{\Gamma}(0)$ can be chosen to be real: [30]

$$A_{if}(0) = \frac{1}{|\mathbf{r}_f - \mathbf{r}_i|^{1/2}} \exp\left(-\frac{|\mathbf{r}_j - \mathbf{r}_i|}{\xi}\right) + \sum_{\alpha} \frac{1}{|\mathbf{r}_{\alpha} - \mathbf{r}_i|^{1/2}} \exp\left(-\frac{|\mathbf{r}_{\alpha} - \mathbf{r}_i|}{\xi}\right) \frac{(\mu_{\alpha})^{1/2}}{|\mathbf{r}_{\alpha} - \mathbf{r}_j|^{1/2}} \exp\left(-\frac{|\mathbf{r}_{\alpha} - \mathbf{r}_j|}{\xi}\right) \quad (7)$$

$$+ \sum_{\alpha, \beta} \frac{1}{|\mathbf{r}_{\alpha} - \mathbf{r}_i|^{1/2}} \exp\left(-\frac{|\mathbf{r}_{\alpha} - \mathbf{r}_i|}{\xi}\right) \frac{(\mu_{\alpha})^{1/2}}{|\mathbf{r}_{\beta} - \mathbf{r}_{\alpha}|^{1/2}} \exp\left(-\frac{|\mathbf{r}_{\beta} - \mathbf{r}_{\alpha}|}{\xi}\right) \frac{(\mu_{\beta})^{1/2}}{|\mathbf{r}_{\beta} - \mathbf{r}_f|^{1/2}} \exp\left(-\frac{|\mathbf{r}_{\beta} - \mathbf{r}_f|}{\xi}\right) + \dots$$

$$= \sum_{\Gamma} A_{\Gamma}(0) \quad (8)$$

$$\mu_{\alpha} \sim \frac{b}{\epsilon_{\alpha} - \epsilon_i} \quad (9)$$

Here μ_{α} is the amplitude of scattering on α 's localized state, ϵ_i and ϵ_{α} are energies of the tunneling electron and the localized scattering state, $b \sim \sqrt{\xi}\epsilon_0 > 0$, and ϵ_0 is the characteristic binding energy of the localized states. Generally ϵ_{α} are random quantities, so the amplitudes $A_{\Gamma}(\mathbf{B} = 0) = A_{\Gamma}(0)$ have random signs. Note that the equation (7) describes both the processes in which an electron is scattered by empty sites and the ones in which it goes through the occupied sites (see Fig. 2) which can be described as a hole moving backwards. The important condition for the interference is that in the final state all intermediate electrons should return to their original positions and spin states.

The hopping probability W_{if} is a random quantity. Generally, to get the value of the resistance of the system one has to solve the full percolation problem with the probability of individual hops given by W_{if} . [1] However, as long as $\ln[\rho(B)/\rho(0)]/\ln\rho(0) \ll 1$ the magnetoresistance is given by the average of the logarithm of the hopping probability [1]:

$$\ln \frac{\rho(B)}{\rho(0)} = - \left\langle \ln \frac{W_{if}(B)}{W_{if}(0)} \right\rangle \quad (10)$$

Here the brackets denote averaging over random scattering configurations and over different hoppings which belong to a percolation cluster. These hoppings are characterized by a typical hopping length, r_{hop} . With a good accuracy, one can replace the full average (10) with the average over random scattering configurations for the hopping processes

by the distance r_{hop} . Physically the averaging of the logarithm in (10) means that the resistivity is controlled by the typical hopping probability, rather than by rare events.

The application of a magnetic field \mathbf{B} introduces random phases to the tunneling amplitudes

$$A_\Gamma(B) = A_\Gamma(0) \exp[i2\pi \frac{\Phi_\Gamma}{\Phi_0}], \quad (11)$$

where $\Phi_\Gamma = BS_\Gamma$, S_Γ is the area enclosed between the path Γ and straight line going from initial to final states, see Fig. 1b.

Depending on distributions of the signs of the amplitudes $A_\Gamma(0)$ the orbital magnetoresistance can be both positive and negative. To illustrate this fact let us consider a model in which there are only two paths, $A_1(0) \sim A_2(0)$, which are independent random quantities and $|\Phi_1 - \Phi_2| \sim \Phi_0$. If $A_{1,2}(0) > 0$ are positive, in the presence of magnetic field, the amplitudes $A_\Gamma(B)$ partially cancel each other. As a result, $\langle \ln W_{ij}(B) \rangle$ decreases by a factor of the order of one when $|\Phi_1 - \Phi_2| \sim \Phi_0$. In this case the magnetoresistance is positive.

The situation changes if $A_{1,2}(0)$ have random signs. In the simplest case when the signs are completely random, the *average* probability $\langle |\sum A_\Gamma(B)|^2 \rangle = \sum \langle |A(0)|^2 \rangle$ is independent of \mathbf{B} . If magnetic flux through the closed loop formed by paths 1 and 2 is larger than the flux quantum, the phases of the amplitudes $A_{1,2}$ are completely random, so that $\langle A_1(B)A_2(B) \rangle = 0$. This implies that the variance $\langle |\sum_\Gamma A_\Gamma(B)|^4 \rangle - \langle |\sum_\Gamma A_\Gamma(B)|^2 \rangle^2$ decreases by a factor of the order of one when $|\Phi_1 - \Phi_2| \sim \Phi_0$. As a result, a typical value of W_{if} defined by (10) increases by a factor of the order of one and the magnetoresistance is negative.

This simplified picture of magnetoresistance being determined by the interference between two paths becomes more complicated for two reasons. First, at large scales the propagation amplitude is dominated by many paths which go through the same scatterer or a group of scatterers. This implies strong correlations between amplitudes A_Γ , as we discuss in section III A. This makes the mathematical problem of calculation of $\rho(B)$ non-trivial. Second, the behavior of the magnetoresistance becomes more complicated if amplitude signs are correlated at some finite distances (see section II C). In this case, one expects a crossover from the negative to positive magnetoresistance as the field is increased, as we explain in section III.

Because the sign and the magnitude of the magnetoresistance are intimately related to the statistics of sign and amplitude distribution of $A_{ij}(0)$ we start with a discussion of this quantity.

B. Statistics of the amplitude A in the absence of the magnetic field.

In the case of small and positive scattering amplitudes, $\mu_\alpha > 0$, and at zero magnetic field the problem of electron tunneling can be mapped [30–33] onto the problem of directed polymers. In the latter problem one studies the thermodynamics of an elastic string in a delta-correlated two dimensional random potential, $W(x, y)$ that is characterized by energy functional

$$H_{dirpol}\{y(x)\} = \int_{-\infty}^x \left[\frac{\sigma}{2} (\partial_x y)^2 + W(x, y(x)) \right] dx \quad (12)$$

Introducing the partition function, $Z(y, x) = \sum_{y\{x\}} \exp(-\beta H)$ of the string that ends at point (x, y) one gets that its evolution as a function of x is described by the equation

$$\partial_x Z = \frac{1}{2\beta\sigma} \partial_y^2 Z - \beta W(x, y) Z. \quad (13)$$

This equation should be compared with the equation for the particle propagation in disordered media:

$$E\Psi = -\frac{1}{2m} \nabla^2 \Psi + V(x, y)\Psi. \quad (14)$$

with white noise potential $V(x, y)$. At negative energies corresponding to tunneling we substitute $\Psi = \exp(-\beta\sigma x)Z(x, y)$; one can neglect second order derivative in x terms that are small at weak potential $V \ll -E$. Then, the Schrodinger equation (14) coincides with (13) with $(\sigma\beta)^2 = -2mE$ and $W = \sigma V/2E$. This mapping also holds for arbitrary (not necessarily white noise correlated) potential V . However, it becomes less useful for arbitrary potentials because analytical results for this problem were obtained only in the case of the white noise potential.

Computation of positive magnetoresistance requires the solution of the directed polymers beyond the white noise approximation, so the analytical results are not directly applicable. Furthermore, the physically relevant problem of

scattering with negative amplitudes cannot be mapped onto any thermodynamic problem because the corresponding free energy becomes imaginary. The applicability of the results of the directed polymer problem in the white noise approximation becomes even more questionable in this case. Below we give a brief review of the results of the directed polymers problem in the white noise approximation. Then we present results of our numerical simulations beyond the white noise approximation, which indicate that these problems belong to the same universality class. Finally, we discuss the statistics of the signs of the tunneling amplitude and show that the existence of the “sign phase transition” is compatible with the results for directed polymer problem.

The main result of the directed polymer theory is the scaling form of the fluctuational part of the free energy of the polymer of length L , $F \propto L^{1/3}$ and its deviations in the transverse direction $Y \propto L^{2/3}$. For equivalent problem of domain wall pinning this scaling was first found numerically in work[34]. Analytically, it was extracted from the third moment of the distribution function of polymers of length L , $\mathcal{P}(F)$. [35, 36] The replica method that was used in this work might be questioned because of an apparent non-commutativity of the limits $L \rightarrow \infty$ and $n \rightarrow 0$ and because it gives unphysical results for all moments of the distribution function except the third. All these problems can be eliminated by solving for the distribution of the energy differences of the infinitely long polymers that end at different points y_1, y_2 , this solution gives the same scaling exponents. [37] as the original approach[34–36, 38–40].

The striking generality of this scaling result that we prove by numerical simulations below is, probably, due to the qualitative reasoning that relates it to the Markovian form of the free energy fluctuations as a function of transverse coordinate. Indeed, The Markovian form implies that free energy fluctuations at large scales are proportional to $Y^{1/2}$, on the other hand they should be of the order of the string elastic energy at these scales: $Y^2/L \propto Y^{1/2}$. Solving the last equation for Y we get the scaling dependencies of the exact solution and of the numerical simulations.

Despite being intuitively appealing, the Markovian nature of free energy fluctuations is difficult to prove for the physically relevant situation in which some scattering amplitudes (9) are very large. It is even more difficult to prove it for the case of rare negative scattering amplitudes in which wave function can change sign at some points. At these points the free energy defined by $F \equiv -T \ln Z$ acquires imaginary part ($\Im F = \pi$) whilst its real part becomes large. Because these points are due to close by negative scatterers, the effective free energy becomes highly correlated which violates the main assumption of the Markovian nature of the free energy fluctuations.

Recently[41, 42], a full Bethe ansatz solution of problem (12) established the complete form of the distribution function of free energy $F \equiv -T \ln Z$ of the string of length L , which turns out to coincide with the Tracy-Widom distribution[43]. This result allows one to check if the problem of particle hopping belongs to the same universality class as the directed polymers. Namely, we define the effective free energy of the quantum problem as

$$F = -\Re \ln A(x, y) \quad (15)$$

where A is the electron amplitude at site (x, y) propagating in x -direction. This free energy describes the decay of the wave function. We compute the amplitude A by simulating electron propagation and check the scaling properties of its real part fluctuations in y -direction and the universality of the distribution function.

We determine the amplitude A from the solution of the lattice recursive equation

$$A_{i,j} = \frac{g}{\epsilon_{ij}} [A_{i-1,j+1} + A_{i-1,j} + A_{i-1,j-1}] \quad (16)$$

where ϵ_{ij} are random independent variables defined on each lattice site and g is the parameter that determines the average decay of the amplitude (inverse localization length). We shall discuss below different distribution functions of ϵ_{ij} appropriate for different physical systems.

Physically, the model (16) describes the motion of electrons on the lattice shown in Fig. 3. The site with energy $\epsilon_{ij} = \langle \epsilon \rangle$ can be identified with ideal lattice, the rest with impurities. If energy ϵ_{ij} is distributed in a narrow interval around its average, the evolution (16) becomes equivalent to (14) in the continuum limit. As discussed in section II A the most physically natural choices of the distribution function of ϵ are uniform $P(\epsilon) = \theta(\epsilon)$, linear $P(\epsilon) = 2\epsilon$ and their analogs for the negative scattering amplitudes: $P(\epsilon) = 1/2$, linear $P(\epsilon) = |\epsilon|$. In all cases we assume that the distribution is cutoff by ϵ_0 at large ϵ : $P(|\epsilon| > \epsilon_0) = 0$. The choice of ϵ_0 determines the average decay rate of the electron amplitude which is mostly irrelevant, in the computations we have set it to $\epsilon_0 = 1$. We have also studied the gapped distribution $P(\epsilon) = 2$ for $1/2 < \epsilon < 1$ for which we expect to get the results similar to the one predicted by exact solution. Finally we studied the binary distribution $P(\epsilon) = (1 - X)\delta(\epsilon - 1) + X\delta(\epsilon - (\mu + 1)^{-1})$ characterized by parameter X and negative scattering amplitude $\mu < 0$.

Some of our results are presented in Figs. 4 and 5. For all studied distribution we observe very good scaling, $\langle \Delta F^2 \rangle^{1/2} \propto L^\gamma$, with the exponents $\gamma = 0.28, 0.345, 0.343$ for gapped, linear and uniform densities of states respectively. These values are very close to the expected value $1/3$, especially for the linear and uniform densities of states. The data for the gapped density of states display a significant transient regime, so the deviation of the

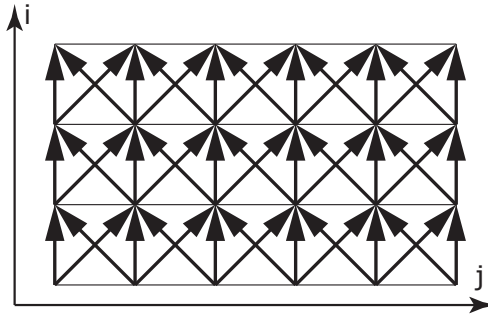


FIG. 3: Schematics of the electron propagation described by equation (16). The computation of the localization length discussed in section IIB involved simultaneous propagation of amplitudes in the vertical direction for many (typically $L > 10^6$) steps. For the computation of the matrix elements in section IIIB the wave functions were assumed to be localized on two sites in the middle of upper and lower rows at distance L and then determined in the middle .

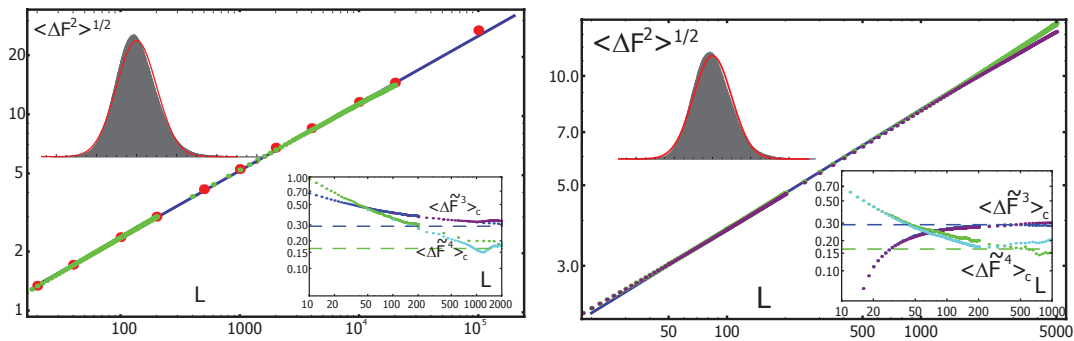


FIG. 4: Scaling dependence of the fluctuations of electron wave function decay, $\Delta F = \langle F \rangle - F$ where F is defined by (15). The quantity F is equivalent to the free energy of the directed polymer problem. The left panel shows the results for the linear density of states with $P(\epsilon < 0) = 0$, the right panel gives the same results for the equally probable positive and negative scattering amplitudes. The upper inserts show the distribution function of ΔF and its fit to the Gaussian compared to which the distribution is slightly skewed as expected for Tracy-Widom distribution. The lower inserts show the evolution of the normalized higher moments of the distribution function that tends to the universal values expected for Tracy-Widom (shown as dashed horizontal lines). The numerical results were obtained by by simulating the evolution (16) on systems of sizes $N = 10^6, 10^7$ and 5×10^7 as indicated by points of different size and colors. The straight line correspond to exponent $\gamma = 0.345$ and 0.33 for left and right panels respectively. The convergence to the scaling form of the free energy fluctuations happens relatively fast while higher moments of the distribution function require enormous statistics, especially at large L as is indicated by the deviation of curves representing fourth moment for $N = 10^7$ and $N = 5 \times 10^7$

exponent from the analytical result is not surprising. The presence of negative scattering amplitudes has small effect on these exponents, they become $\gamma = 0.31, 0.33, 0.345$ that are even closer to the expected values. Furthermore, the higher moments of the distribution function tend to the universal values expected for the Tracy-Widom distribution. These results is in agreement with the works[44, 45] that observed Tracy Widom distribution of conductances in two dimensional models.

These data lead to the conclusion that the main results of the directed polymer problem, namely, the scaling dependence of the free energy and the universality of the distribution function remain valid for the problem of electron tunneling in disordered media.

C. The sign phase transition.

As explained in section II A, the sign of the magnetoresistance is related to the statistics of signs of amplitudes $A_{if}(0)$ in the absence of magnetic field. If the concentration of impurities with negative scattering amplitudes is large, the sign of $A_{if}(0)$ becomes completely random. If all impurities are characterized by positive scattering amplitudes $\mu_i > 0$, the sign of $A_{if}(0)$ is positive. Let us denote the probability to find a positive amplitude $A_{if}(0)$ by P_+ and

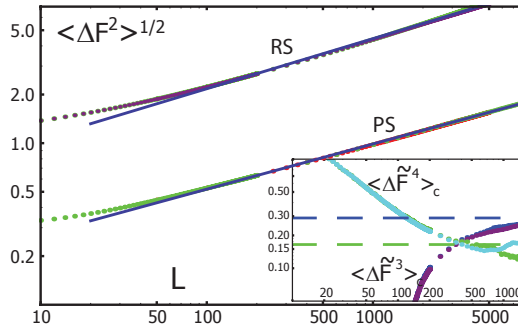


FIG. 5: Scaling dependence of the fluctuations of electron wave function decay, $\Delta F = \langle F \rangle - F$ obtained from the numerical solution of the evolution (16) with gapped density of states. The lower data set (denoted PS) correspond to the positive scattering amplitudes, the upper data set (denoted RS) to the completely random amplitudes with equal probability of signs. The data were fit with the scaling dependencies with the exponent $\gamma = 0.28$ for positive scatterers and $\gamma = 0.31$ for random signs. The results were obtained for the systems of size $N = 10^7$ and 5×10^7 . Higher moments tend to the universal values of Tracy-Widom distribution as shown in the insert that gives the data for random sign scatterers.

negative by P_- . The quantity $\Delta P = P_+ - P_-$ characterizes the sign order. As the concentration, X , of the impurities with negative scattering amplitudes increases, ΔP should change from 1 to 0. Generally, ΔP is scale dependent and acquires its limiting value at $|r_i - r_f| \rightarrow \infty$. There are two logical possibilities: either at large scales $\Delta P_{r \rightarrow \infty} = 0$ only for $X > X_c$ while for smaller $X < X_c$ $\Delta P_{r \rightarrow \infty} > 0$, or that any non-zero $x > 0$ leads to $\Delta P_{r \rightarrow \infty} = 0$. The former implies that the change in the x -dependence of the sign statistics can be viewed as a phase transition. This possibility has been suggested in [24, 25, 27], the alternative was argued for in works [31–33].

Here we study the sign statistics in the lattice models defined by (16) in section IIB and show that both the phase transition and crossover can be realized depending on the distribution of ϵ . We start with the simplest case of binary distribution $P(\epsilon) = (1 - X)\delta(\epsilon - 1) + X\delta(\epsilon + \epsilon_0)$ with small $X \ll 1$ and small $\epsilon_0 \ll 1$. This model describes the wave function propagation on the ideal lattice (sites with $\epsilon = 1$) which contains rare impurities characterized by a negative scattering amplitude $\mu \approx -1/2\epsilon_0, |\mu| \gg 1$. The large value of $|\mu|$ allows a continuous description of the tunneling amplitude. The size of the region where the tunneling amplitude $A_{if}(0) < 0$ is negative may be found by noticing that the wave function

$$\Psi(x, y) = \exp(-x/\xi) + \frac{\mu}{(x^2 + y^2)^{1/4}} \exp(-\sqrt{x^2 + y^2}/\xi)$$

changes its sign in the egg-shaped region in the wake of the impurity given by:

$$y^2(x) = x\xi \ln[\mu^2/x], \quad 0 < x < \mu^2.$$

The area of this region is

$$S(\mu) = \frac{2}{3} \sqrt{\frac{2\pi}{3}} |\mu|^3 \xi^{1/2}.$$

A small concentration, $XS \ll 1$ of such impurities leads to independent lakes of negative signs shown in Fig. 6. In this situation $\Delta P > 0$.

As the concentration x is increased, different lakes start to overlap and form a state with random sign of the amplitudes. The transition between these two phases takes place at $X = X_c \sim S^{-1} \propto |\mu|^{-3}$. The dependence $P_-(X)$ is expected to have a general form characteristic of a phase transition sketched in Fig. 7a. These qualitative arguments ignore the contributions from impurities located close to each other which should not be relevant in the limit $X \rightarrow 0$.

The numerical simulations show that the transition survives for not so large values of the scattering amplitudes as well. In particular, this has been observed for the binary distribution functions with $\epsilon_0 = 1$. Fig. 7 represents the results of our numerical simulations for this case. As one can see, the behavior of ΔP as a function of the distance changes qualitatively as one increases X beyond $X_c \approx 0.032$. For smaller concentrations, x , probability difference ΔP saturates at non-zero values, whilst for larger concentrations it approaches 0. The scales needed to observe this change in the behavior are generally very long. We believe that this is the reason that prevented establishing unambiguously the existence of the transition in early numerical simulations. We note that the scales are further enlarged near $X_c \approx 0.032$ as one expects at a phase transition.

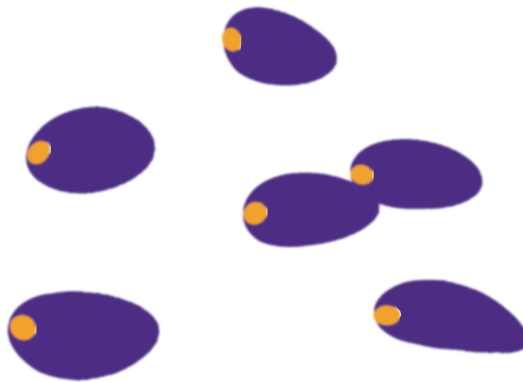


FIG. 6: Qualitative picture of lakes of negative amplitude signs formed in the wake on an impurity (shown as a small yellow circle) characterized by negative scattering amplitude

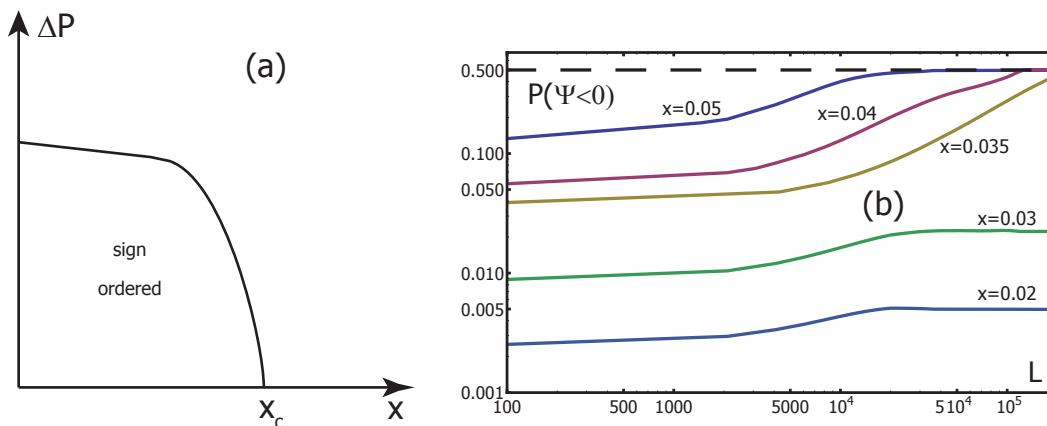


FIG. 7: Panel a: Qualitative picture of the phase transition described by the order parameter defined $\Delta P(X)$ that happens at $X_c \approx 0.032$ for the the binary distribution described in the text. Panel b: Scale dependence of the probability of negative amplitude that shows the transition around $X_c \approx 0.032$.

We have also checked that the phase transition between the sign ordered and sign disordered phases survives for a gapped distribution of ϵ defined in section II B. The numerical data look very similar to those shown in Fig. 7, the expected value of X_c in this model is $X_c \approx 0.02$.

The existence of the sign phase transition has been questioned in paper [33] which used the mapping to the directed polymer problem. The essence of the argument is that the free energy of directed polymers leading to a given site are dominated by a single path, so that just a single impurity along this path suffices to change the sign of the amplitude. At a small concentration of negative scatterings, one concludes that the amplitude should become completely random at the scale $L \propto 1/X$. This argument, however, does not take into account the contribution from subdominant paths that may eventually restore the sign of the amplitude at large scales as is indicated by numerical data for the gapped density of states, see section II B.

We now show that for a gapless density of states (3) with $\beta < 2$ and for any non-zero concentration of negative scatterers the sign of the amplitude A becomes completely random at large scales. Indeed, in this case the total area of negative lakes is

$$S_{tot} \sim X \int d\epsilon \nu(\epsilon) S[\mu(\epsilon)]$$

where $S[\mu] \propto \mu^3 \propto \epsilon^{-3}$. Thus, S_{tot} diverges for all densities of states $\nu(\epsilon) \sim \epsilon^\beta$ with $\beta \leq 2$. This is the case for example in the case of Coulomb gap where $\nu(\epsilon) \propto \epsilon$.

We have checked this conclusion numerically for the linear density of states and we have indeed observed that even

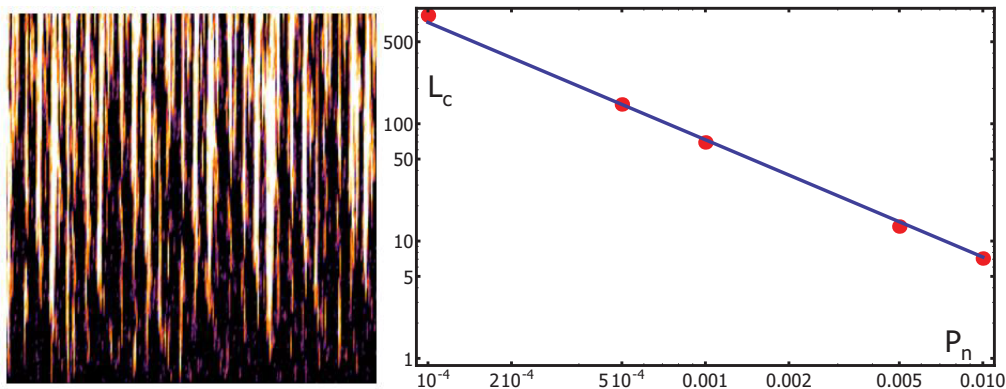


FIG. 8: The map of the amplitude sign resulting from the wave function evolution in vertical direction for the linear density of states. The wave function has all positive signs (shown in black) in the beginning of the evolution (bottom). As the evolution goes upward the presence of a small concentration, $X = 10^{-4}$, of negative scattering amplitudes results in a larger and larger regions of negative signs (white regions) until the whole amplitude sign becomes completely random at the top. The right panel shows the length scale $L(X)$ at which the sign becomes random as a function of the concentration X . Here we defined $L(X)$ as the length at which $\Delta P = 0.25$. The data are well fit with the dependence $L \propto 1/X$ in agreement with the theoretical expectations based on directed polymer mapping.

a very small $X \sim 10^{-4}$ leads to a random sign of the amplitude at very large scales. Our data are shown in Fig. 8. As expected, the scale at which the sign becomes random grows quickly with the decrease of X .

III. MAGNETORESISTANCE IN HOPPING REGIME.

A. Magnetic field dependence of the localization length.

We now turn to the discussion of magnetoresistance in the variable hopping regime. We begin by summarizing the results of numerical simulations for the recursive equation (16) that was modified to include the phases, $\phi_j = Bj$, induced by magnetic field

$$A_{i,j}(B) = \frac{1}{\epsilon_{ij}} [A_{i-1,j-1} e^{i\phi_{j-1/2}} + A_{i-1,j} e^{i\phi_{j-1/2}} + A_{i-1,j+1} e^{i\phi_{j+1/2}}]. \quad (17)$$

Then we give the qualitative explanation of the results based on the mapping to the directed polymer problem. The dimensionless magnetic field B in this equation and in the discussion below is given by the flux of the physical magnetic field, B_{phys} , through the elementary square Malplaquet of the lattice: $B = B_{phys} a^2 / \Phi_0$ where a is the lattice constant and $\Phi_0 = hc/e$ is the flux quantum.

Our main result is that at large $r_{hop} > L_B$ (which holds at low temperatures), both positive and the negative magneto resistances are described by corrections to the localization length:

$$g(B) = \frac{\Delta \xi(B)}{\xi(0)} = \pm C_{\pm} \left(\frac{B \xi^2}{\Phi_0} \right)^{\alpha}. \quad (18)$$

This scaling law is characterized by the universal exponent $\alpha \approx 4/5$ and non-universal numerical coefficients C_{\pm} . The latter depends on the distribution of ϵ_{ij} , e.g. $C_+ \approx 2.6$ for the gaped and $C_+ \approx 0.9$ for linear density of states. Here we define the localization length as the limiting behavior of the amplitude $\xi = \lim_{r_{ij} \rightarrow \infty} \ln A_{ij}(B) / r_{ij}$. The positive sign (+) in (18) corresponds to the case where the system is in the sign disordered phase, the negative sign corresponds to the sign ordered phase. The universal regime (18) is achieved at low fields. Notice that whilst the value of $\xi(B)$ is mathematically defined for any magnetic field, its applicability to the hopping problem requires that $r_{hop} > L_B$.

At intermediate fields one often observes a slightly different power law

$$g(B) = \frac{\Delta \xi(B)}{\xi(0)} = \pm D_{\pm} \left(\frac{B \xi^2}{\Phi_0} \right)^{\alpha'} \quad (19)$$

with a different exponent and prefactors, $\alpha' \approx 0.5, 0.6, 0.64$ for the scattering of random signs with gaped, linear and uniform densities of states respectively. For these densities of states the prefactors are $D_+ \approx 0.11, 0.22, 0.30$.

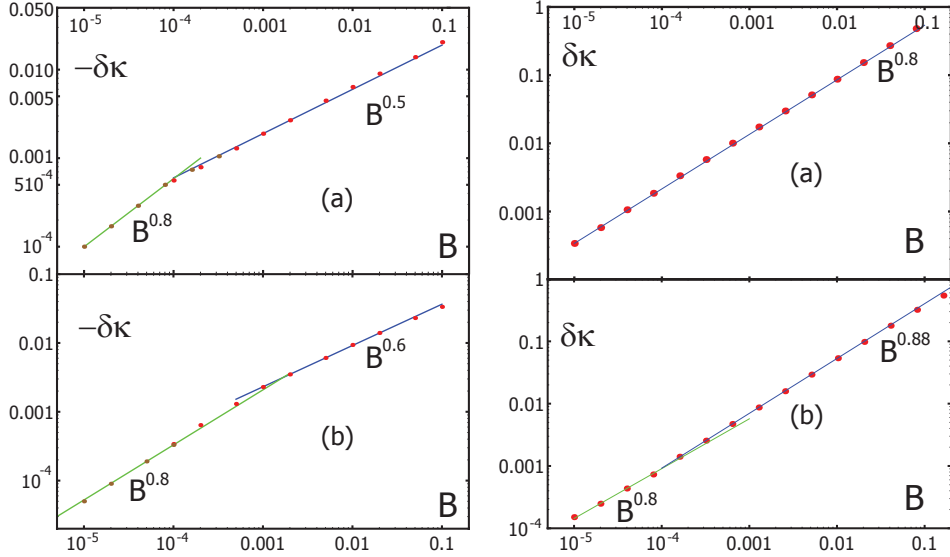


FIG. 9: Change in the inverse correlation length, $\delta\kappa = \delta(1/\xi)$ induced by magnetic field. The upper panels correspond to the gapped density states, the lower panels correspond to linear density states. The left panels correspond to random scattering amplitude signs, the right one+ to positive scattering. The absolute values of inverse correlation length at $B = 0$ in these cases are $\xi_0^{-1} = 1.85, 1.42$ for gapped and linear densities of states, $X = 0.5$ and $\xi_0^{-1} = 1.31, 0.95$ for uniform and linear density of states for positive scattering ($X = 0$). The results for the constant density of states (not shown) are very similar to the ones for the linear density of states shown in lower panels: they display large intermediate regime of power law behavior with exponents 0.6 and 0.9 for $X = 0.5$ and $X = 0.0$ respectively.

The value of D_+ for the gapped density of states is in agreement with the numerical simulations of the previous workers [26, 28]. Note that the value of D_+ for the uniform density of states is roughly three times larger than that for the gapped one. This makes it possible to observe large negative magnetoresistance experimentally as we discuss in section V. These statements are illustrated in Figs. 9. The scaling dependence with the exponent $\alpha' \approx 0.6$ was observed previously in a number of works[28, 32] in which insufficient system sizes prevented the observation of the asymptotic behavior.

We now give qualitative arguments that reproduce the observed scaling behavior of the change in the localization length explained above.

As we have shown in section IIB, the problem of electron tunneling belongs to the same universality class as the problem of directed polymers. In particular, the typical tunneling action varies from one path to another by the amount that scales as $\Delta F \propto L^{1/3}$. This means that the tunneling from point i to f is dominated by a narrow bundle of paths as shown in Fig. 10. The width of this bundle does not increase with the length of the path, so the magnetic field has very little effect on the tunneling in this approximation. Another bundle of paths that differs from the dominant one at scale L has action that is typically larger than that of the dominant path by $\Delta F \propto L^{1/3}$, so its amplitude is exponentially suppressed by $\exp[-c(L/a)^{1/3}]$. Here a is the mean free path of the electron (lattice spacing in the case of numerical simulations). This leads to an exponentially small effect of magnetic field. However, because the difference of the actions between two paths is a random variable itself, with probability $p \propto L^{-1/3}$ two actions differ only by the amount of the order of unity. If all scattering amplitudes are positive, the change in the interference caused by magnetic field decreases the total amplitude by the factor of the order of unity, provided that the flux through the loop formed by these two paths is of the order of the flux quantum. Because the transverse direction scales as $Y \sim a(L/a)^{2/3}$ the interference becomes relevant at scales

$$BL^{5/3}a^{1/3} \sim \Phi_0 \quad (20)$$

with probability $p \sim (L/a)^{-1/3}$. The resulting decrease of the wave function implies that the typical inverse correlation length increases by

$$\delta\xi^{-1} \sim a^{1/3}/L^{4/3} \sim (B/\Phi_0)^{4/5}a^{3/5}$$

Repeating the same arguments for the case of the amplitudes of the random signs and using the fact that the signs of two paths that contribute to the interference are random (cf. discussion after equation (11)), we get the same dependence on magnetic field but with the opposite sign: the inverse correlation length is decreased by magnetic field.

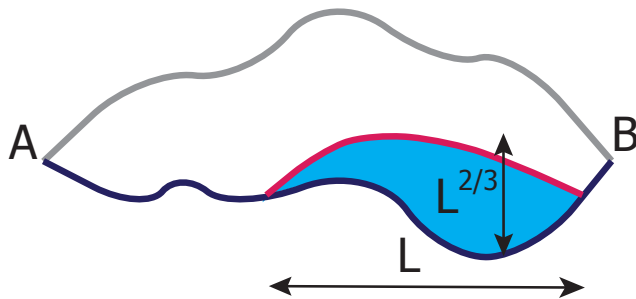


FIG. 10: Directed polymer picture

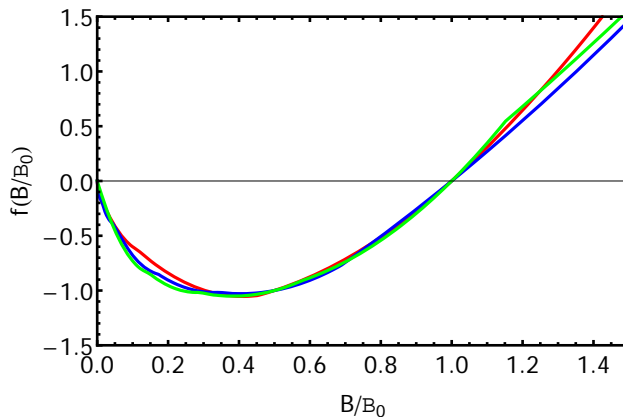


FIG. 11: Universal behavior of the increment of the inverse localization length as a function of the field for small concentration of negative ϵ_{ij} and linear density of states. Different curves show $\delta\xi^{-1}$ for different concentrations $X = 0.02, 0.08$ and 0.16 rescaled in both vertical and horizontal directions: $\delta\xi^{-1} = \delta\xi_0^{-1}\chi(B/B_0)$. The characteristic value of the field scales with X : $B_0 \propto X^\beta$ with $\beta \approx 2.8$ (insert). Very small values of the field imply that negative correction of $\delta\xi^{-1}$ wins over positive only when signs are completely randomized, even a small correlation between the signs of the amplitude is sufficient to result in the positive correction.

All these conclusions are valid in the limit of long scales where $\Delta F \gg 1$. In the intermediate regime, in which $\Delta F \lesssim 1$ the probability that two paths interfere is of the order of unity resulting in the scaling dependence of $\delta\xi^{-1}$ on the field with the exponent $\alpha' = 3/5$. Looking at the numerical results for the scaling dependence of ΔF shown in Fig. 4 we see that it remains of the order of unity for $L \lesssim 10^2$ which translates into the field $B \gtrsim 10^{-3}$ in rough agreement with the numerical results shown in Fig. 9.

The behavior of the correlation length is given by the simple scaling equations (18,19) only in the limit of completely random and positive amplitude signs. In the case of a small concentration of negative scatterings one expects a more complicated behavior. Large fields affect amplitude at short scales. At these scales the rare negative scatterings have small effect on the amplitude sign, so at large fields the inverse localization length is increased by the field, similarly to the case of positive scattering amplitudes. In contrast, at large scales relevant for small fields the amplitude sign becomes completely random, so at small fields one expects a negative correction to $\delta\xi^{-1}$, similar to a fully random sign case. As the field is increased, the sign of the correction should change. Exactly this qualitative behavior is shown by numerical simulations of the model (17) with a small concentration of scatterers with negative amplitudes. Our results shown in Fig. 11 display universal behavior of $\delta\xi^{-1}(B/B_0)$. The characteristic field B_0 scales, as expected, with concentration X : $B_0 \propto X^\beta$, however, the value of exponent $\beta \approx 2.8$ is sufficiently larger than one would expect from the scaling behavior of $L(x) \propto 1/x$ obtained in section II C: $\beta_{expected} \approx 1.6$. We do not have a satisfactory explanation of this discrepancy. We only note that very small values of B_0 found numerically imply that even a small amount of sign correlations is sufficient to result in the positive $\delta\xi^{-1}$. This is not so surprising because positive increment of $\delta\xi^{-1}$, although given by the same scaling dependence, is order of magnitude larger than the negative one (cf. right and left panels of Fig. 9).

The scaling dependence (18) is non-analytic in B , so it should dominate over other sources of corrections to the localization radius at $B \rightarrow 0$. In the electron hopping problem the largest scale, r_{hop} , for the coherent electron

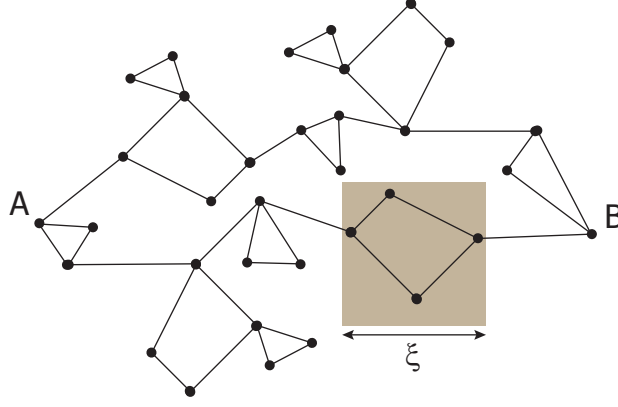


FIG. 12: Quantitative picture of the tunneling paths in the vicinity of metal insulator transition when $\xi > a_B$. The path may contain return loops at short scales (of the order of ξ) but at longer scales the electron moves only in one directions. We expect that the problem is mapped onto directed polymers at scales larger than ξ , so that small magnetic fields $B\xi^2 \lesssim \Phi_0$ are expected to have the same effect on the resistivity as the in the strongly localized regime.

tunneling is set by temperature (1). The non-analytic behavior predicted by (18) takes place provided that the scale L given by (20) is less than $r_{hop}(T)$:

$$(\Phi_0/B)^{3/5} a^{1/5} < \xi \left(\frac{T_0}{T} \right)^\zeta.$$

In the discussion of the hopping transport we have assumed the strongly localized regime in which the electron wave function is localized at the scales of the order of the Bohr radius, a_B of a single impurity. However, all our qualitative conclusions should also hold when localization length is larger, $\xi > a_B$. In this case the electrons tunnel from one area to another as shown in Fig. 12. The loops of the tunneling paths are allowed inside individual areas, but not between them. In this regime one expects to observe large non-analytic dependence of the localization length on magnetic field given by (18,19) at low fields $B\xi^2 \lesssim \Phi_0$. These universal corrections adds to the effect of magnetic field coming from the scales shorter than ξ that may be found from the renormalization group approach. These corrections are of the order of $\delta\xi/\xi \sim (B\xi^2/\Phi_0)^2$ and thus are negligible compared to the effects (18,19) coming from the longer scales at low fields. They can, however, contribute significantly to the total variation of the magnetoresistance at large fields.

B. Magnetoresistance in variable range hopping regime.

The results (18,19) for the $\xi(B)$ dependence can be converted into magnetoresistance provided that the induced change of the localization length is small $\delta\xi \ll \xi$, but the resulting change in the hopping amplitude is exponentially large leading to resistance variations $\ln(\rho(0)/\rho(B)) \gg 1$. In this case one can neglect other contributions to the variation of the hopping probability (that we discuss below) so that magnetoresistance is given by

$$\ln \left[\frac{\rho(B)}{\rho(0)} \right] \approx \left[2\zeta \left(\frac{T_0}{T} \right)^\zeta \right] \frac{\delta\xi}{\xi} \quad (21)$$

Combined with the $\xi(B)$ dependence discussed in section III A this equation gives the magnetoresistance at moderate fields, so that $B\xi^2 \lesssim \Phi_0$ but $\ln(\rho(0)/\rho(B)) \gg 1$.

At large magnetic fields $B\xi^2 \gtrsim \Phi_0$ the equation (21) remains valid but the localization length dependence on magnetic field is due to short scales and is non-universal. For a granular metal the localization length is roughly equal to the grains size r_0 ; because the magnetic field has no effect at scales shorter than r_0 , $\delta\xi(B)$ dependence saturates at $B\xi^2 \lesssim \Phi_0$. In contrast, in the case of a weakly disordered non-interacting 2D metal with $kl_{tr} > 1$ one expects[7] strong dependence on magnetic field. Indeed, in this case the localization length is exponentially large $\xi(0) \sim l_{tr} \exp(k_F l_{tr})$ in the absence of magnetic field, l_{tr} being electron mean free path. The conventional renormalization group analysis[7] gives $\delta\xi(B)/\xi(0) \sim (B\xi^2/\Phi_0)^2$ at $B\xi^2 < \Phi_0$, so one expects corrections of the order of unity at $B\xi^2 \approx \Phi_0$. At larger

fields ($Bl_{tr}^2 \sim \Phi_0$) the localization length increases exponentially to $\xi(B) \sim l_{tr} \exp(k_F l_{tr})^2$. At even larger fields one expects the appearance of the quantum Hall regime and a pseudometallic behavior.[13] The presence of electron-electron interaction can lead to even larger variety in the localization length dependence on magnetic field at high fields.

The computation of $\xi(B)$ dependence in section III A translates into the predictions for magnetoresistance (21) only in the asymptotic regime of large magnetic field at which $\ln(\rho(0)/\rho(B)) \gg 1$. There are at least two reasons why it is important to study the magnetoresistance in the opposite limit of low magnetic field.

First, because it is difficult to measure large resistances, the parameter $r/\xi \lesssim 15$ cannot be very large, so the condition is $\ln(\rho(0)/\rho(B)) \gg 1$ is satisfied only in a limited range of fields. As we show below, the power law dependence of $\ln(\rho(0)/\rho(B))$ extends somewhat in the regime if $\ln(\rho(0)/\rho(B)) \lesssim 1$ which makes the observation of this dependence more realistic.

Second, many data show that the magnetoresistance often changes sign in small fields. As we discuss in more detail below, this sign change agrees with the theoretical expectations. For instance, if the scattering amplitudes are mostly positive ($P_- \ll 1$) the localization length at large fields becomes shorter (see section II C) and magnetoresistance is positive. However, at small fields it may change its sign and become negative. This change in the sign of the magnetoresistance can be due to the change in the sign of the correction to the localization length discussed in section II Cor to another effect at short scales that we discuss below. Generally, the theoretical predictions in this regime are less universal.

At small magnetic field the accuracy of the approximation $M_{ij} \sim A_{ij}$ becomes insufficient because it overestimates contributions to the hopping rate (4) from the impurity configurations in which the partial amplitudes $A_\Gamma(0)$ cancel each other in the absence of magnetic field, so that the value of $A_{if}(0) \approx 0$. For these configurations a small magnetic field changes $\ln A_{if}$ dramatically. For a finite probability density of $A_{ij}(0) = 0$ the magnetic field dependence of $\overline{\ln A(B)}$ becomes a non-analytic function of B : $\overline{\ln[A(B)/A(0)]} \propto |B|$. [24, 25] Similarly to the qualitative discussion of $\xi(B)$ dependence in section III A this non-analyticity can be demonstrated in the case when propagation amplitude is due to the interference between just two paths: $A_{if} = A_1 + A_2 \approx 0$ with random A_1 and A_2 . In this model case the typical amplitude in magnetic field becomes

$$\overline{\ln \left| \frac{A(B)}{A(0)} \right|} = \int dA_1 dA_2 \ln |A_1 - A_2 e^{i\phi}| \sim |\phi| \quad (22)$$

where $\phi \propto B$ is the phase difference induced by the magnetic field. Here and below we denote by bar the averaging over the impurity configurations. Because the probability density of $A_{ij}(0) = 0$ is finite at any concentration of scatterers with $\mu_i < 0$, the typical amplitude always grows at small fields. This however does not *always* translate into negative magnetoresistance.

The crucial difference between the amplitude A_{ij} and the hopping rate (4) is that the latter is the sum of the positive rates due to phonons with different q directions. As a result, the probability density to find $W_{if} = 0$ is zero, and at small B the magnetoresistance is proportional to B^2 .

In order to find the values of the crossover fields we note that in the limit of low temperatures at which $qr_{ij} \ll 1$ the exponential in (5) can be approximated by the first non-zero term:

$$M_{ij}(\vec{q}) \sim \int d\vec{r} \psi_i^\dagger(\vec{r}) \psi_j(\vec{r}) \vec{q} \vec{r}. \quad (23)$$

The main contribution to the matrix element M_{ij} comes from the components of the phonon wave vector \vec{q} which is parallel to \vec{r}_{ij} . In the leading approximation we can neglect the contributions from the phonons with momenta in other directions. In this approximation the hopping probability (4) is controlled by the matrix element $M_{ij}(q\hat{r}_{ij})$ $\hat{r}_{ij} = \vec{r}_{ij}/r_{ij}$. This matrix element has the same statistical properties as the amplitude A_{if} , so the reasoning resulting in (22) applies and $\overline{\ln |M(B, \vec{q})/M(0, \vec{q})|} \sim |B|$. The subleading processes in which the hopping (4) is due to phonons with momenta perpendicular to \vec{r}_{ij} cut off the non-analytic behavior of $\overline{\ln W(B)}$ at very small fields.

Combining this result with the effect of $\xi(B)$ dependence discussed in section III A that takes place at large scales at which the flux through the typical loop is larger than the flux quantum, $B r^{5/3} \xi^{1/3} > \Phi_0$, we get three regimes of the $\overline{\ln M(B)}$ dependence for $B \xi^2 < \Phi_0$:

$$\ln \frac{\rho(0)}{\rho(B)} = \overline{\ln \frac{W_{if}(B)}{W_{if}(0)}} \sim \begin{cases} (B/B_0)^\alpha \gtrsim 1 & B > B_0 \\ |B|/B_0 \lesssim 1 & B_0 > B > B_* \\ B^2/(B_* B_0) \ll 1 & B < B_* \end{cases} \quad (24)$$

where $B_0 = \Phi_0/r^{5/3}\xi^{1/3}$. As we saw in section III A the transverse deviations of the typical path scale as $r_\perp \sim r^{2/3}\xi^{1/3}$. This allows us to estimate the contribution to the average (4) from phonons with $q \perp r$: $W_\perp \sim (\xi/r)^{2/3}W$. Repeating

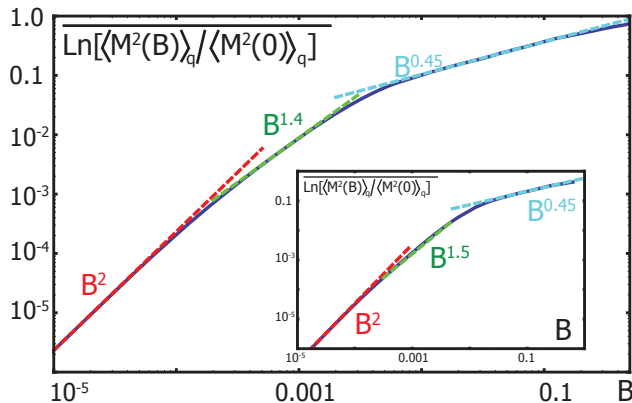


FIG. 13: Phonon matrix element as a function of magnetic field at long and moderate scales. The main panel shows field dependence of the matrix element for relatively long hops for which corresponding to $r/\xi \approx 8.0$. One observes a very significant (two decades) regime of the pseudo-universal scaling dependence associated with the localization length dependence (19). At shorter scales (corresponding to $r/\xi \approx 6$ shown in the insert) the scaling regime shrinks. In both cases the regime of analytical dependence (B^2) is limited to very small fields.

the arguments that led to (22) we get

$$\overline{\ln \frac{W(B)}{W(0)}} = \int dW_{\parallel} \ln [W_{\parallel} + W_{typ} \phi^2 + W_{\perp}] \quad (25)$$

that results in the dependence (25) with $B_* = \Phi_0/r^2$.

The qualitative estimates show that while the regime of non-analytic dependence is relatively wide ($B_0 < B < \Phi_0/r^2$) the regime of the linear dependence is narrow. We note that the estimates of B_* and B_0 neglect the numerical coefficients that might be important.

The discussion above and the result (24) assumed that the system is deep in the sign disordered phase in which signs of all amplitudes are completely random. If the scattering amplitudes are mostly positive $P_- \ll 1$ the signs of the amplitudes become random only at large scales. It implies that the system may be in the sign ordered phase at characteristic scales set by magnetic field. In this case the magnetoresistance at largest fields is positive in contrast to (24), while at small B it is quadratic in B , so it can be both positive and negative depending on the value of $P_- \ll 1$.

To check the validity of (25) for realistic parameters we have performed the numerical computation of the matrix elements. We did not attempt a full computation of the matrix element and its averaging over the distribution of r_{ij} that characterize the percolating cluster. Instead, we computed matrix element for the characteristic r_{ij} and averaged over different direction of q . Because the results do not change qualitatively when r is increased by a factor of 2, we believe that they reproduce faithfully the dependence of the magnetoresistance:

$$\ln(\rho(0)/\rho(B)) = \overline{\ln \left[\langle M^2(B) \rangle_q / \langle M^2(0) \rangle_q \right]} \quad (26)$$

where angular brackets denote averaging of the directions of \vec{q} . The result of our numerical simulations for the case of uniform density of states $P(\epsilon) = (1/2)\theta(1 - |\epsilon|)$ is shown in Fig. 13 for two typical distances: $r/\xi \approx 8$ and $r/\xi \approx 6$. In both cases one observes a large regime of the pseudo-universal behavior $\ln(\rho(0)/\rho(B)) \sim B^\alpha$ with $\alpha \approx 0.5$ that is due to the non-universal corrections to the localization length (19). At larger $r/\xi \gtrsim 8$ one observes the gradual appearance of the transient linear dependence in magnetic field in agreement with the expectations (25). Figure 14 shows expected magnetoconductance at different typical values of r/ξ converted into expected values of the resistances.

C. Beyond the single particle model.

So far in our discussion we have ignored the many body effects due to electron-electron interaction. Generally one expects that electron correlations play much bigger role in the hopping regime than in the metallic regime. In this subsection we briefly discuss their role, and the conditions under which the single particle results obtained above are valid.

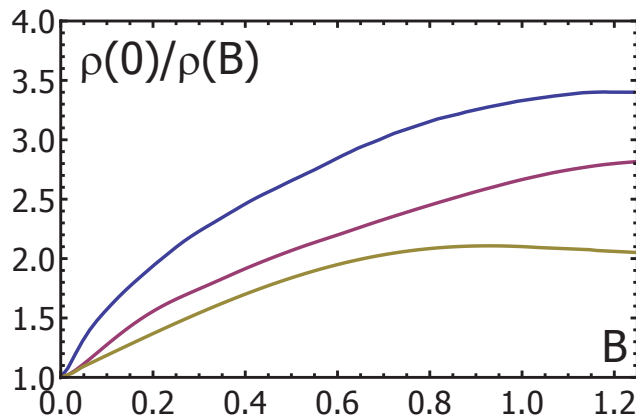


FIG. 14: Magnetoconductance as a function of magnetic field for different values of the matrix element at zero field corresponding to $R_{\square}/R_Q \approx 5 \cdot 10^5$, $1.0 \cdot 10^4$, $1.0 \cdot 10^3$. For small matrix elements (large resistances) the behavior at low fields can be approximated by a power law $\sigma(B)/\sigma(0) \approx B^a$ with $a \approx 0.5 - 0.6$. The regime of very small magnetic fields is hardly observable on the linear scale of the plot even for smallest resistances.

At low temperatures the electron sites with $\epsilon_{\alpha} < 0$, (and $\mu_{\alpha} < 0$), are occupied by electrons, while the sites with $\epsilon_{\alpha} > 0$ are empty. Tunneling between initial and final states may be viewed as a virtual process in which the electron hops through the intermediate localized states. Depending on the ratio between the electron-electron interaction and the density of states at the Fermi energy in the impurity band, these localized states can be singly and doubly occupied. The spins in the singly occupied states interact via the exchange interaction, J . Although the detailed theory of the disordered electron systems does not exist, three obvious limiting cases are clearly possible. In the first case, the interaction between electrons is large, so the majority of sites are singly occupied, and the resulting spin system might form a $S = 1/2$ spin glass at low temperatures and a paramagnet at high temperatures. The low temperature spin glass state breaks the time reversal symmetry, it might be collinear or isotropic depending on the anisotropy of the exchange couplings. Although logically possible, neither collinear nor isotropic states were observed experimentally, probably because quantum spin fluctuations are too large for spin $1/2$. The alternative (second case) is that each spin forms a singlet with another spin to which it is coupled by the strongest interaction [46]. This state does not break the time reversal symmetry. Finally, in the limit of small interaction the majority of states are doubly occupied (third case). Both the second and third cases are characterized by zero average spin on each site.

In all cases the segments of the tunneling path where electrons travel through occupied sites may be viewed as a tunneling of a hole moving backwards through occupied states as it is schematically shown in Fig. 2. In the interacting system this process may lead to the creation of many body excitations in the final state that destroy the coherence between hopping amplitudes A_{Γ} along different paths Γ . When it does not happen, the tunneling may be described by the equation (7) with renormalized hopping amplitudes and energies ϵ_a .

We now discuss the tunneling interference in different electron states in more detail. We start with a state in which all sites are single occupied. At high temperatures the resulting spins form a paramagnet, so the final spin state formed after the charge transport along different paths Γ are generally different, and do not coincide with the initial state. In this state the corresponding amplitudes A_{Γ} do not interfere. In this situation one expects no orbital effects of the magnetic field on the charge transport. Application of magnetic field can polarize the spin system, restoring the path interference. Thus, in this case one expects that the polarization of the spin system by the in-plane field results in a state characterized by a large negative magnetoresistance with respect to the field perpendicular to the plane, while application of a small perpendicular field in the absence of in-plane one gives small or no negative magnetoresistance. Large out-of-plane field (in the absence of in-plane field) has two effects: it might polarize the spin system and cause orbital effects. Thus, one expects a complicated behavior as a function of the out-of-plane field.

At low temperatures the spins may freeze in a spin glass state or form a spin liquid. If the spins freeze in the collinear spin glass state, the final states corresponding to two paths mostly coincide and the interference reappears. In this situation the electron hopping amplitude can be described by essentially the same equation (7). Thus, one expects the same orbital effect of the magnetic field, as discussed in section III A.

The electron hopping becomes very different in the non-collinear spin glass because the electron amplitudes acquire a non-trivial phase factors due to spin non-collinearity which can be described by complex scattering amplitudes μ_a . We expect that magnetic field does not affect the interference in this case and does not lead to orbital magnetoresistance. However, the isotropic spin glass state is rather unlikely to be realized in physical two and even three dimensional

glasses.[47]

In contrast to the spin glass states, the spin singlets formed in the second and third cases do not break the time reversal symmetry. Thus, the scattering amplitudes in these situations remain real as in the single particle model. At low temperatures the final states formed after charge motion should coincide, so the interference between different paths remains the same as it was in the one particle model of section III A.

We do not discuss here the effect of magnetic field on the spin configuration which also affects the transport of charges. This discussion is beyond the scope of this paper devoted to the orbital effects. We, however, mention briefly possible scenarios in section V where we discuss the experiment that indicates that these effects are important.

IV. APPLICATION TO OTHER PHYSICAL SYSTEMS.

The sign phase transition that appears for binary distribution of scattering amplitudes discussed in section II C can be observed in very different physical systems. Here we show that it affects the physics of random classical magnets at high temperatures. The simplest example is given by the Ising model on a cubic lattice

$$H = \sum_{ij} J_{ij} s_i s_j \quad (27)$$

where $s_i = \pm 1$ and the exchange interactions takes two values: $J_{ij} = J_0 > 0$ with probability $(1 - X)$ and $J_{ij} = J_0$ with probability X respectively.

At high temperatures the susceptibility in this model

$$\chi(\mathbf{r}_i, \mathbf{r}_f) = \langle s(\mathbf{r}_i) s(\mathbf{r}_f) \rangle = \sum_{\{s_0\}} s(\mathbf{r}_i) s(\mathbf{r}_f) \exp\left(-\frac{H}{T}\right) \quad (28)$$

which is random quantity at large $r_{if} \gg 1$. To show the existence of sign phase transition in this quantity we notice that at $T \gg |J_{ij}|$ one can expand the exponent in (28) and take into account only directed paths between sites i and f . The sum over directed path is equivalent to solution of the recursion equation

$$\chi_{km} = \chi_{k-1m} J_{k-1m}^{km} + \chi_{i,m-1} J_{km-1n}^{km} \quad (29)$$

Here indices (km) denote the site with coordinates k, m on the square lattice and J_{k-1m}^{km} denote the bond connecting two such sites. The recursion (29) is very similar to (16) with binary distribution of ϵ_{ij} , so one expects that it shows the same sign transition as function of concentration, X , of negative bonds. The only difference between (29) and (16) is that in the former the negative signs are associated with bonds and in the latter with sites. This is similar to the difference between site and bond disorder in percolation problem which is known to have very little effect. Thus, we expect that at $r \rightarrow \infty$ the distribution function of $\chi(r)$ exhibits the sign phase transition as a function of X . At high temperatures the critical value X_c is T -independent. As the temperature is decreased, the sign correlations increase which can lead to the formation of the sign ordered phase. This means that the transition from spin disordered to spin ordered phase shifts to larger X at lower temperatures. Finally, at sufficiently low temperatures the system might become a ferromagnet. At the transition point the susceptibility (28) decreases as a power law of $|r_i - r_f|$ and the sign correlations are long ranged whereas spin correlator decreases exponentially. Thus, the transition to the sign ordered state happens above the transition to a ferromagnet.

The staggered susceptibility is defined by $\tilde{\chi}(r) = (-1)^n \chi(r)$, where n is the number of steps in a direct path on square lattice between the sites 0 and r . Obviously it also exhibits a sign phase transition. Thus, at high temperatures the sign disordered phase is separated from the phases in which the sign of the susceptibility is positive or alternating. At sufficiently low temperatures the system freezes into a magnetically ordered or a spin glass phase. The spin glass phase may be sign ordered or disordered, the former corresponds to the coexistence of ferromagnetic (or antiferromagnetic) and spin glass order parameters. These conclusions are summarized by the phase diagram shown in Fig. 2.

V. REVIEW OF THE EXPERIMENTAL RESULTS AND CONCLUSIONS.

Theoretical expectations described in the previous sections can be separated into the qualitative and quantitative predictions. Verification of the qualitative prediction of the orbital mechanism of a large negative magnetoresistance in the variable range hopping regime is relatively simple: requires only measurements of the anisotropy with respect

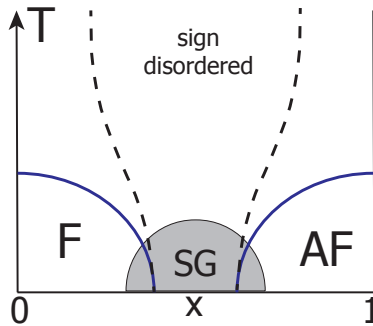


FIG. 15: Qualitative picture of a phase diagram of Ising spin glass. Dashed lines separate sign ordered and sign disordered phases at high temperatures. The spin glass phase (shown in gray) appears in dimension three and higher. In two dimensions the spin system remains paramagnetic down to lowest temperatures in the absence of the ferro- (or antiferro-) magnetic long range order.

to the parallel and perpendicular magnetic field. In contrast, to verify quantitative predictions represented by (18,19) would require stronger conditions $\ln[\varrho(0)/\rho(B)] > 1$, and $B\xi^2 > \Phi_0$. We are not aware of experiments on the negative magnetoresistance where all these requirements were satisfied. Below we discuss currently available data on large negative magnetoresistance in the variable range hopping.

We begin with the maximal value of the magnetoresistance observed experimentally and expected theoretically. In our numerical simulations we got the maximal value of $\delta\xi/\xi = 0.2$ for the uniform (Mott regime) and $\delta\xi/\xi = 0.05$ for the linear in ε (Efros-Shklovskii regime) density of states. The measurable values of the resistance ($R \lesssim 10^{11} \Omega$) correspond to $(T_0/T)^\zeta \lesssim 15$. Thus (18,19) describe the negative magnetoresistance whose value does not exceed $\varrho(0)/\rho(B) < 30$ in the Mott regime, and is expected to be more moderate, $\ln[\varrho(0)/\rho(B)] < 1$, in Efros-Shklovskii regime. This is in agreement with the fact that in all works [8–18] where both the large negative magnetoresistance has been observed and the temperature dependence of the resistance has been measured, it followed Mott’s law.

Surprisingly, one of the most comprehensive studies of the negative magnetoresistance in the variable range hopping regime in a two dimensional material was done in the early work[8] that studied *Ge*-sopped *GaAs* films. It observed a strongly anisotropic negative magneto resistance, the largest one corresponding to the out-of-plane field. The effect of the in-plane field can be accounted for by a significant thickness of the film ($d_{eff} \approx 30nm$). Moreover, the in-plane negative magneto resistance was also anisotropic with respect to the angle between the magnetic field and the current. Finally, microscopic fluctuations of the resistance as a function of the magnetic field in small samples was observed. These observations prove the orbital nature of the effect. In this experiment the resistance of the sample was $R_\square \lesssim 30M\Omega$ at lowest temperatures indicating that $r/\xi \lesssim 5$. Accordingly the magnitude of the negative magneto resistance remained moderate: $(\rho(0) - \rho(B))/\rho(0)_{max} \sim 0.4$. In Fig. 16 we present results of our numerical simulations of the equation (26) and their comparison with the experimental data of [8]. The work[10] observed negative magneto resistance with similar amplitude and similar dependence on magnetic field in thin films of polycrystalline In_2O_{3-x} .

A subsequent work [9] on $GaAs/Al_xGa_{1-x}As$ disordered hetero junctions observed significantly larger negative magneto resistance $\varrho(0)/\rho(B) \sim 7$. Strong anisotropy of the negative magneto resistance has been observed indicating the orbital nature of the effect. The magnetic field dependence of $\rho(B)$ in low fields $B \lesssim 4T$ where magneto resistance is negative was roughly linear in coordinates $\ln \rho(B)$, $B^{1/2}$ which is in a good agreement with the dependence expected theoretically (25) and shown in Fig. 14. In these experiments the localization length varied between $\xi = 25 - 100 nm$ for different gate voltages, so that $B\xi^2 \sim \Phi_0$ occurs at $B \sim 4T$. Generally one expects that the magneto conductance should show a crossover to a different regime when $B\xi^2 \sim \Phi_0$. It is surprising that this crossover is not observed in the data. On the other hand, this work and works discussed below give values for the localization length ξ extracted from the Mott law. This procedure is prone to a number of uncertainties such as the value of the density of states, the exact form of the temperature dependence, etc, so the values of the localization length might be wrong by a factor 2 – 5 which would be sufficient to explain the absence of the crossover in [9]. Similar large negative magneto resistance ($\varrho(0)/\rho(B) \sim 20$) of orbital nature has been observed in polycrystalline In_2O_{3-x} films in[11]. The behavior of $\varrho(0)/\rho(B)$ in these experiments resembles a small power of magnetic fields in a wide range of fields for all fields, the quadratic behavior was observed only in very low fields ($B < 0.2T$), at which the relative change in the resistance was very small $\delta R/R \ll 1$ in agreement with the theoretical expectations (cf. Fig. 13 in which B^2 behavior appears at $\delta R/R \lesssim 10^{-2} - 10^{-1}$).

The maximal value of magnetoresistance in works [9–11] is somewhat above the one expected theoretically for the

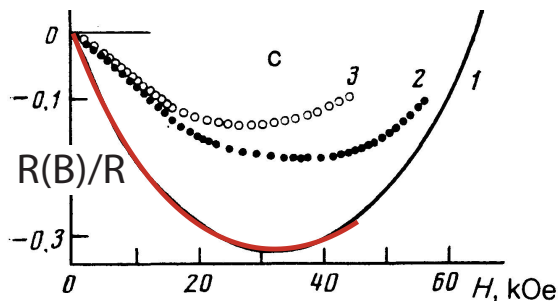


FIG. 16: Data from [8] and their fit to the behavior of (18) expected for relatively small resistances $R_{\square}/R_Q \approx 10^3 - 10^4$ that used the matrix elements computed in section III B. The lower data curve correspond to the field perpendicular to the plane of the sample. The middle data points show the effect of the field in plane of the sample perpendicular to the direction of the current, the highest data set to the field in the direction of the current. The upturn at the large fields is due to the effect of the field at small scales where it modifies the hopping amplitude between the sites which was not taken into account properly in the model.

films of these resistances. For instance, the resistance of GaAs/Al_xGa_{1-x}As films in work [9] implies that at the lowest temperature the maximal value of $(T_0/T)^{1/3} \approx 7$ for these films which translates into the maximal expected value for $\rho(0)/\rho(B) \sim 2 - 3$. It is possible, however, that the largest fields studied in these works correspond to the regime $B\xi^2 \gtrsim \Phi_0$ in which the magnetoresistance may continue to grow with B .

Huge effect of the transverse field on the conductivity ($\rho(0)/\rho(B) \gtrsim 30$) of high mobility silicon MOSFET was observed [12, 13] at low carrier concentrations. Remarkably in these experiments the large magnetoresistance in the transverse field appears only when the spins are polarized by large in-plane field whilst low fields result in an isotropic small and positive magnetoresistance. The latter indicates its spin nature which is in agreement with the strong correlations expected in this material. As discussed in section III C this implies the existence of the localized spins in the system that suppresses the orbital effect of the magnetic field. Application of a large in-plane field polarizes the spins making the path interference possible, so that a transverse field added to the system leads to a large negative magnetoresistance, as observed experimentally. Unfortunately, the work [12] did not study the temperature dependence of the resistivity in these samples. It is likely that the change of the sign of magnetoresistance observed in work [14] that studied the pregraphitic carbon nanofibers that obey Efros-Shklovskii law is due to a similar mechanism. Unfortunately, this work did not study the field anisotropy.

The paper [15] reported a big negative magnetoresistance ($\rho(0)/\rho(B) \sim 10$) of the H-doped graphene, whilst in-plane field had practically no effect on the resistance. The observed negative magnetoresistance can be interpreted as a large change in the localization length: $\xi(B)/\xi(0) = 4$ induced by $B = 9$ T field. These results cannot be compared directly with the universal scaling dependence derived in this work because the large changes in the localization length imply that $B\xi^2 \sim 1$. One expects that at lower temperatures the samples studied in this work should exhibit large magnetoresistance at low fields associated with small $\delta\xi/\xi$ but these data are not available.

Finally, it is possible that negative magnetoresistance due to orbital effect was observed in other materials as well but not studied in any detail. For instance, the work [16] observed a sharp (factor of 2) drop of resistance in fields $B = 1$ T at $T = 100$ mK for CdSe: In samples that display three dimensional Mott resistance with exponent $\zeta = 1/4$ and $R(0) = 6$ M Ω cm, significant ($\delta G/G \sim 0.2$) negative magnetoresistance was also observed in three dimensional doped n-type InP samples that also show Mott law but much lower resistance $R(0) \sim 10$ Ω cm. The paper [17] reported decrease of the resistance by a factor of 100 in the field $B = 1$ T for Ge films at $T = 36$ mK characterized by $R = 400$ k Ω .

The complexity of the data outlined above shows that they cannot be explained solely by a single particle theory. In particular, it cannot explain why some materials exhibit only positive while others only negative magnetoresistance in whole range of temperatures and magnetic fields in the variable range hopping regime. Moreover, there are also materials that exhibit an isotropic positive magnetoresistance only at small fields. At larger in-plane fields the magnetoresistance of these samples saturates, and addition of a small perpendicular field results in a giant negative magnetoresistance [12, 13]. Evidently, the spin physics plays an important role in the these materials.

Positive magnetoresistance of several orders of magnitude in high magnetic field has been observed in many experimental works, see e.g. [23, 48, 49]. However, no data set is sufficiently complete to allow one to associate it with the orbital interference mechanisms [19] described by (18,19). For example, these works did not study the anisotropy of the magnetoresistance.

We now briefly discuss the origin of the isotropic positive magnetoresistance in small fields which was observed in a number of works. There are at least three possibilities. The first one is that the electron spin polarization increases the electron energy. As a result, the density of states at the Fermi energy changes as well. This is expected to be a

relatively small effect. An alternative mechanism associates it with the presence of both singly and doubly occupied states near the Fermi energy in the impurity band. In the absence of magnetic field the process in which the electron hops from one occupied site to another (creating a singlet) is possible. Magnetic field polarizes spins which suppresses such processes [50]. Thus the magnetic field effectively changes the density of states in the impurity band. This mechanism provides quadratic in B contribution to $\log \sigma$. Therefore, it can be effective only in the absence of the orbital contribution, which is non-analytic in B .

A different mechanism might be effective if the electron system is strongly correlated, and in the absence of disorder is close to the Wigner-crystal-Fermi liquid transition. In the presence of disorder, the system may be visualized as a random mixture of crystal and liquid puddles. In this case the insulating phase corresponds to the situation where metallic puddles do not overlap. Because the magnetic susceptibility of the Wigner crystal is higher than that of the Fermi liquid, the fraction of the Wigner crystal grows with increasing magnetic field leading to the positive magnetoresistance [13]. In the theory of ${}^3\text{He}$ this phenomenon is known as the Pomeranchuk effect. It is possible that huge positive isotropic magnetoresistance observed in [12, 13, 51] in the metallic regime of Si MOSFET's and GaAs quantum wells is due to this mechanism. We believe that the same mechanism may be responsible for the positive isotropic magnetoresistance in the hopping regime [13].

Finally, the spin alignment in the parallel field produces the interference between the paths and corresponds to a new mechanism of magnetoresistance. Though this mechanism in the hopping regime has never been considered theoretically, it is clear that it also produces a negative magnetoresistance. We expect that this contribution will be isotropic.

While this work was in progress we learned about work[52] that gives the arguments for the universal corrections to the magnetoresistance of strongly disordered superconductors described by a model similar to the electron hopping discussed here. In our terminology this model corresponds to the case of the uniform density of states and positive scattering amplitudes.

Acknowledgments. We acknowledge useful discussions with M. Feigelman, J. Folk, X.P.A. Gao, M. Gershenson, D. Huse, S. Kravchenko, I. Sadovskyy, M. Sarachik and B.I. Shklovskii. B.S. thanks the International Institute of Physics (Natal, Brazil) for hospitality during the completion of the paper. This research was supported by grants ARO W911NF-09-1-0395, ANR QuDec and John Templeton Foundation. The opinions expressed in this publication are those of the author(s) and do not necessarily reflect the views of the John Templeton Foundation and Templeton

-
- [1] A. L. Efros and B. I. Shklovskii, in *Electron-electron interactions in disordered systems*, edited by A. Efros and M. Pollak (North Holland, 1985), vol. 10 of *Modern Problems in Condensed Matter Sciences*, chap. 5, p. 409.
 - [2] N. F. Mott, *Metal-insulator transitions* (Taylor and Francis, 1990).
 - [3] A. A. Abrikosov, *Fundamentals of the Theory of Metals* (North Holland, 1988).
 - [4] B. L. Altshuler, P. A. Lee, D. Khmel'nitzkii, and A. I. Larkin, *Physical Review B (Condensed Matter)* **22**, 5142 (1979), URL <http://dx.doi.org/10.1103/PhysRevB.22.5142>.
 - [5] S. Hikami, A. I. Larkin, and Y. Nagaoka, *Progress of Theoretical Physics* **63**, 707 (1980).
 - [6] A. I. Larkin, *Pis'ma v Zhurnal Eksperimental'noi i Teoreticheskoi Fiziki* **31**, 239 (1980).
 - [7] P. A. Lee and T. V. Ramakrishnan, *Reviews of Modern Physics* **57**, 287 (1985), URL <http://dx.doi.org/10.1103/RevModPhys.57.287>.
 - [8] E. I. Laiko, A. O. Orlov, A. K. Savchenko, E. A. Il'ichev, and E. A. Poltoratskii, *Soviet Physics - JETP* **66**, 1258 (1987).
 - [9] H. W. Jiang, C. E. Johnson, and K. L. Wang, *Physical Review B (Condensed Matter)* **46**, 12830 (1992), URL <http://dx.doi.org/10.1103/PhysRevB.46.12830>.
 - [10] F. P. Milliken and Z. Ovadyahu, *Physical Review Letters* **65**, 911 (1990), URL <http://dx.doi.org/10.1103/PhysRevLett.65.911>.
 - [11] A. Frydman and Z. Ovadyahu, *Solid State Communications* **94**, 745 (1995), URL [http://dx.doi.org/10.1016/0038-1098\(95\)00141-7](http://dx.doi.org/10.1016/0038-1098(95)00141-7).
 - [12] S. V. Kravchenko, D. Simonian, M. P. Sarachik, A. D. Kent, and V. M. Pudalov, *Physical Review B (Condensed Matter)* **58**, 3553 (1998), URL <http://dx.doi.org/10.1103/PhysRevB.58.3553>.
 - [13] B. Spivak, S. V. Kravchenko, S. A. Kivelson, and X. P. A. Gao, *Reviews of Modern Physics* **82**, 1743 (2010), URL <http://dx.doi.org/10.1103/RevModPhys.82.1743>.
 - [14] Y. Wang and J. J. Santiago-Aviles, *Applied Physics Letters* **89**, 123119 (2006), URL <http://dx.doi.org/10.1063/1.2338573>.
 - [15] X. Hong, S.-H. Cheng, C. Herding, and J. Zhu, *Physical Review B* **83**, 085410 (2011), URL <http://dx.doi.org/10.1103/PhysRevB.83.085410>.
 - [16] J. R. Friedman, Y. Zhang, P. Dai, and M. P. Sarachik, *Physical Review B (Condensed Matter)* **53**, 9528 (1996), URL <http://dx.doi.org/10.1103/PhysRevB.53.9528>.

- [17] V. F. Mitin, V. K. Dugaev, and G. G. Ihas, *Applied Physics Letters* **91**, 202107 (2007), URL <http://dx.doi.org/10.1063/1.2813615>.
- [18] F. Hellman, M. Q. Tran, A. E. Gebala, E. M. Wilcox, and R. C. Dynes, *Physical Review Letters* **77**, 4652 (1996), URL <http://dx.doi.org/10.1103/PhysRevLett.77.4652>.
- [19] B. I. Shklovskii, *JETP Lett* **36**, 51 (1982).
- [20] B. I. Shklovskii and A. L. Efros, *Soviet Physics - JETP* **57**, 470 (1983).
- [21] A. V. Khaetskii and B. I. Shklovskii, *Soviet Physics - JETP* **58**, 421 (1983).
- [22] B. I. Shklovskii, *Soviet Physics - Semiconductors* **17**, 1311 (1983).
- [23] B. I. Shklovskii and A. L. Efros, *Electronic Properties of Doped Semiconductors* (Springer, 1984).
- [24] V. L. Nguen, B. Z. Spivak, and B. I. Shklovskii, *Soviet Physics - JETP* **62**, 1021 (1985).
- [25] B. I. Shklovskii and B. Z. Spivak, in *Hopping and Related Phenomena* (Singapore, Singapore, 1990), pp. 139 – 50.
- [26] E. Medina, M. Kardar, Y. Shapir, and X. R. Wang, *Phys. Rev. Lett.* **64**, 1816 (1990), URL <http://dx.doi.org/10.1103/PhysRevLett.64.1816>.
- [27] B. I. Shklovskii and B. Z. Spivak, in *Hopping transport in solids*, edited by M. Pollak and B. Shklovskii (Elsevier, 1991), vol. 28 of *Modern Problems in Condensed Matter Sciences*, chap. 9, pp. 271–348.
- [28] H. L. Zhao, B. Spivak, M. P. Gelfand, and S. Feng, *Physical Review B (Condensed Matter)* **44**, 10760 (1991), URL <http://dx.doi.org/10.1103/PhysRevB.44.10760>.
- [29] V. L. Nguen, B. Z. Spivak, and B. I. Shklovskii, *JETP Letters* **43**, 44 (1986).
- [30] B. I. Shklovskii and B. Z. Spivak, *Journal of Statistical Physics* **38**, 267 (1985).
- [31] E. Medina and M. Kardar, *Phys. Rev. B* **46**, 9984 (1992), URL <http://link.aps.org/doi/10.1103/PhysRevB.46.9984>.
- [32] E. Medina, M. Kardar, and R. Rangel, *Physical Review B (Condensed Matter)* **53**, 7663 (1996), URL <http://dx.doi.org/10.1103/PhysRevB.53.7663>.
- [33] H. Kim and D. A. Huse, *Physical Review B (Condensed Matter and Materials Physics)* **83**, 052405 (2011), URL <http://dx.doi.org/10.1103/PhysRevB.83.052405>.
- [34] D. Huse and C. Henley, *Physical Review Letters* **54**, 2708 (1985), URL <http://dx.doi.org/10.1103/PhysRevLett.54.2708>.
- [35] M. Kardar and Y.-C. Zhang, *Physical Review Letters* **58**, 2087 (1987), URL <http://dx.doi.org/10.1103/PhysRevLett.58.2087>.
- [36] M. Kardar, *Nuclear Physics B, Field Theory and Statistical Systems* **B290**, 582 (1987).
- [37] V. S. Dotsenko, L. B. Ioffe, V. B. Geshkenbein, S. E. Korshunov, and G. Blatter, *Physical Review Letters* **100**, 050601 (2008), URL <http://dx.doi.org/10.1103/PhysRevLett.100.050601>.
- [38] M. Kardar, D. Huse, C. Henley, and D. Fisher, *Physical Review Letters* **55**, 2923 (1985), roughening;Ising model;impurities;finite temperatures;random coupling energies;numerical simulations;fluctuations;energy gain;exponents;lattice;free energy;, URL <http://dx.doi.org/10.1103/PhysRevLett.55.2923>.
- [39] M. Kardar and D. Nelson, *Physical Review Letters* **55**, 1157 (1985), URL <http://dx.doi.org/10.1103/PhysRevLett.55.1157>.
- [40] M. Kardar, G. Parisi, and Y. C. Zhang, *Physical Review Letters* **56**, 889 (1986), URL <http://dx.doi.org/10.1103/PhysRevLett.56.889>.
- [41] P. Calabrese, P. Le Doussal, and A. Rosso, *Europhysics Letters* **90**, 20002 (2010), URL <http://dx.doi.org/10.1209/0295-5075/90/20002>.
- [42] V. Dotsenko, *Europhysics Letters* **90**, 20003 (2010), URL <http://dx.doi.org/10.1209/0295-5075/90/20003>.
- [43] C. Tracy and H. Widom, *Communications in Mathematical Physics* **159**, 151 (1994).
- [44] A. Somoza, M. Ortuno, and J. Prior, *Physical Review Letters* **99**, 116602 (2007), URL <http://dx.doi.org/10.1103/PhysRevLett.99.116602>.
- [45] J. Prior, A. Somoza, and M. Ortuno, *The European Physics Journal B* **70**, 513 (2009), URL <http://dx.doi.org/10.1140/epjb/e2009-00244-x>.
- [46] R. N. Bhatt and P. A. Lee, *Physical Review Letters* **48**, 344 (1982), URL <http://dx.doi.org/10.1103/PhysRevLett.48.344>.
- [47] K. H. Fischer and H. J. A., *Spin Glasses* (Cambridge University Press, 1993).
- [48] I. Shlimak, A. Ionov, and B. I. Shklovskii, *Soviet Physics - Semiconductors* **17**, 314 (1983).
- [49] A. N. Ionov, I. S. Shlimak, and M. N. Matveev, *Solid State Communications* **47**, 763 (1983), URL [http://dx.doi.org/10.1016/0038-1098\(83\)90063-7](http://dx.doi.org/10.1016/0038-1098(83)90063-7).
- [50] H. Kamimura, in *Electron-electron interactions in disordered systems*, edited by A. Efros and M. Pollak (North Holland, 1985), vol. 10 of *Modern Problems in Condensed Matter Sciences*, chap. 7, p. 555.
- [51] X. P. A. Gao, G. S. Boebinger, A. P. Mills, A. P. Ramirez, L. N. Pfeiffer, and K. W. West, *Physical Review B (Condensed Matter and Materials Physics)* **73**, 241315 (2006), URL <http://dx.doi.org/10.1103/PhysRevB.73.241315>.
- [52] A. Gangopadhyay, V. Galitski, and M. Mueller, *Magnetoresistance of an anderson insulator of bosons* (2012), URL <http://arxiv.org/abs/1210.3726>.